Primary resistance to PD-1 blockade mediated by *JAK1/2* mutations

Daniel Sanghoon Shin[1], Jesse M. Zaretsky[1], Helena Escuin-Ordinas[1], Angel Garcia-Diaz[1],

Siwen Hu-Lieskovan[1], Anusha Kalbasi[1], Catherine S. Grasso[1], Willy Hugo[1], Salemiz Sandoval[1],

Davis Y. Torrejon[1], Nicolaos Palaskas[1], Gabriel Abril Rodriguez[1], Giulia Parisi[1], Ariel Azhdam[1],

Bartosz Chmielowski[1,2], Grace Cherry[1], Elizabeth Seja[1], Beata Berent-Maoz[1], I. Peter Shintaku[1],

Dung Thi Le[3], Drew M. Pardoll[3], Luis A. Diaz, Jr[3], Paul C. Tumeh[1], Thomas G. Graeber[1,2],

Roger S. Lo[1,2], Begoña Comin-Anduix[1,2], Antoni Ribas[1,2]

[1]University of California Los Angeles (UCLA), Los Angeles, CA, USA.

[2]Jonsson Comprehensive Cancer Center, Los Angeles, CA.

[3]Johns Hopkins Sidney Kimmel Comprehensive Cancer Center, Baltimore, MD.

*Correspondence to: Antoni Ribas, MD, PhD, Department of Medicine, Division of Hematology-

Oncology, UCLA, 11-934 Factor Building, 10833 Le Conte Avenue, Los Angeles, CA 90095-

1782. Phone: 310 206 3928, Email: aribas@mednet.ucla.edu.

Running Title: Primary Resistance to PD-1 blockade

Key Words: Melanoma, PD-1 blockade, interferon signaling, tumor resistance to immune response

Disclosures: Daniel Sanghoon Shin, Jesse M. Zaretsky, Angel Garcia-Diaz and Antoni Ribas have submitted an institutional invention report on the role of JAK1/2 mutations and resistance to anti-PD-1 therapy. Paul C. Tumeh is a full time employee of Acteris Inc. The other authors do not have conflicts of interest to report.

Abstract

Loss of function mutations in *JAK1/2* can lead to acquired resistance to anti-programmed death

protein 1 (PD-1) therapy. We reasoned they may also be involved in primary resistance to anti-

PD-1 therapy. *JAK1/2* inactivating mutations were noted in tumor biopsies of 1 of 23 patients

with melanoma and in 1 of 16 patients with mismatch repair deficient colon cancer treated with

PD-1 blockade. Both cases had a high mutational load but did not respond to anti-PD-1 therapy.

Two out of 48 human melanoma cell lines had *JAK1/2* mutations, which led to lack of PD-L1

expression upon interferon gamma exposure mediated by inability to signal through the

interferon gamma receptor pathway. *JAK1/2* loss-of-function alterations in TCGA confer adverse

outcomes in patients. We propose that *JAK1/2* loss-of-function mutations are a genetic

mechanism of lack of reactive PD-L1 expression and response to interferon gamma, leading to

primary resistance to PD-1 blockade therapy.

Significance

A key functional result from somatic *JAK1/2* mutations in a cancer cell is the inability to respond

to interferon gamma by expressing PD-L1 and many other interferon-stimulated genes. These

mutations result in a genetic mechanism for the absence of reactive PD-L1 expression, and

patients harboring such tumors would be unlikely to respond to PD-1 blockade therapy.

3

Introduction

Blocking the programmed death 1 (PD-1) negative immune receptor results in unprecedented rates of long lasting anti-tumor activity in patients with metastatic cancers of different histologies, including melanoma, Hodgkin's disease, Merkel cell, head and neck, lung, esophageal, gastric, liver, kidney, ovarian, bladder and high mutational load cancers with defective mismatch repair, among others in a rapidly growing list (1-8). This remarkable anti-tumor activity is explained by the reactivation of tumor antigen-specific T cells that were previously inactive due to the interaction between PD-1 and its ligand PD-L1 expressed by cancer cells (1, 9-12). Upon tumor antigen recognition, T cells produce interferon gamma, which through the interferon gamma receptor, the Janus kinases JAK1 and JAK2 and the signal transducers and activators of transcription (STATs) results in the expression of a large number of interferon-stimulated genes. Most of these genes lead to beneficial antitumor effects, such as increased antigen presentation through inducible proteasome subunits, transporters associated with antigen processing (TAP) and the major histocompatibility complex (MHC), as well as increased production of chemokines attracting T cells and direct tumor growth arrest and apoptosis (13). However, interferon gamma also provides the signal that allows cancer cells to inactivate antitumor T cells by the adaptive expression of PD-L1 (9), thereby specifically escaping their cytotoxic effects (12).

Acquired resistance to PD-1 blockade in patients with advanced melanoma can be associated with loss-of-function mutations with loss of heterozygosity in *JAK1/2* or in beta 2-microglobulin (*B2M*) (14). The complex genetic changes leading to acquired resistance to PD-1 blockade, wherein one *JAK1/2* allele was mutated and amplified and the other was lost, suggest a strong selective pressure induced by the therapeutic immune response. Similar events leading to lack of sensitivity to interferon gamma have been reported in the cancer immune-editing process and

4

acquired resistance to immunotherapy in mouse models (15-17) and in patients treated with the anti-CTLA-4 antibody ipilimumab who did not respond to therapy (18). Therefore, lack of interferon gamma responsiveness allows cancer cells to escape from antitumor T cells, and in the context of anti-PD-1/L1 therapy, results in the loss of PD-L1 expression, the target of PD-1 blockade therapy, which would abrogate the antitumor efficacy of this approach.

In order to explore the role of *JAK1* and *JAK2* disruption in primary resistance to PD-1 blockade therapy, we performed a genetic analysis of tumors from patients with melanoma and colon cancer who did not respond to PD-1 blockade therapy despite having a high mutational load. We identified tumors with homozygous loss of function mutations in *JAK1* and *JAK2* and studied the functional effects of deficient interferon gamma receptor signaling that lead to a genetically-mediated absence of PD-L1 expression upon interferon gamma exposure.

5

Results

JAK Loss of Function Mutations in Primary Resistance to PD-1 Blockade in Patients with Metastatic Melanoma

Recent data indicates that tumors with high mutational burden are more likely to have clinical responses to PD-1 blockade therapy (6, 19-21). However, in all of these series some patients fail to respond despite having a high mutational load. We performed whole exome sequencing in 23 pre-treatment biopsies from patients with advanced melanoma treated with anti-PD-1 therapy, which included 14 patients with a tumor response by irRECIST criteria and 9 without a response (Supplementary Table 1). Even though the mean mutational load was higher in responders than non-responders, as reported for lung, colon and bladder cancer (6, 19, 21), some patients with a tumor response had a low mutational load and some patients without a tumor response had a high mutational load (Fig. 1A).

We then assessed whether loss-of-function mutations in interferon receptor signaling molecules, which would prevent adaptive expression of PD-L1, might be present in tumors with relatively high mutational load that did not respond to therapy. A melanoma biopsy from the patient with the highest mutational load among the 9 non-responders (patient #15) had a somatic P429S missense mutation in the src-homology (SH2) domain of *JAK1* (Fig. 1B). Whole exome sequencing of an early passage cell line derived from this tumor (M431) showed an amplification of chromosome 1p, including the *JAK1* locus, and a 4:1 mutant:wild-type allele ratio was observed at both the DNA and RNA level (Supplementary Fig. 1A-E and Supplementary Database 1). None of the tumors from the other 22 patients had homozygous loss-of-function mutations or deletions in the interferon receptor pathway. Rather, the other *JAK2* mutations found in biopsies of responders had low variant allele frequency as shown in Fig. 1B, and were likely heterozygous. These mutations would not carry the same functional

6

significance, as signaling would still occur upon interferon exposure through the wild-type JAK protein from the non-mutated allele. Two non-responders had *IFNGR* mutations, also of low allele frequency and therefore uncertain significance. We also analyzed potential mutations in genes involved in the antigen presenting machinery and did not find any loss of function mutations that were homozygous (Supplementary Fig. 2).

As expected, tumors from patients who responded had a higher density of CD8 cells and PD-L1 in the center and invasive tumor margin (Fig. 1C and D). In contrast, the baseline biopsy from patient #15 with a high mutational load but with the *JAK1* (P429S) missense mutation had undetectable CD8 infiltrates, PD-1 and PD-L1 expression (Supplementary Fig. 3). The amplification of *PD-L1*, *PD-L2* and *JAK2* (PDJ amplicon), which has been associated with a high response rate in Hodgkin's disease (4), was noted only in patient #16 who did not respond to PD-1 blockade therapy despite having the second highest mutational load and a high level of PD-L1 expression (Fig. 1B, D and E).

Functional Analyses of the Role of *JAK* Loss of Function Mutations in Regulating PD-L1 Expression

We next sought to characterize the interferon response of M431, the melanoma cell line established from a biopsy of patient #15 with high mutational load and no response to therapy. First, we optimized flow cytometry conditions in selected human melanoma cell lines (Supplementary Figs. 4A-F, 5A-D, 6A-H, and 7A-C). PD-L1 expression increased less than 1.5 fold interferon gamma exposure in M431 (Fig. 2A), versus 5.1 fold with in M438, used as a positive control cell line established from patient #8 in this same series. pSTAT1 was induced at 30 minutes in M431 but the signal dissipated at 18 hours, faster than in cell lines with more durable responses to interferon gamma leading to PD-L1 upregulation (Fig. 2B, C compared

7

with Supplementary Fig. 8A-C). These data are consistent with the 4:1 *JAK1* mutant:wild type

allele frequency in the M431 cell line (Supplementary Fig. 1A-E).

We then screened a panel of 48 human melanoma cell lines for absolute absence of PD-L1

induction by either type I (alpha and beta) or type II (gamma) interferons. Among the three

interferons, interferon gamma most potently induced PD-L1 expression (Fig. 2D and

Supplementary Fig. 9A and 9B for type I interferons). Two cell lines had *JAK1/2* homozygous

loss of function mutations and did not respond to interferon gamma with upregulation of surface

PD-L1 expression. M368 had a mutation in *JAK2* (20 out of 22 reads, variant allele frequency

0.91) that is predicted to disrupt and shift the D313 splice site acceptor in exon 8 by one

nucleotide, changing the reading frame, and had loss of the wild type allele (Fig. 3A and

Supplementary Fig. 10A and 10B). M395 had an inactivating *JAK1 D775N* kinase domain

mutation in exon 17 and loss of the other allele (140 out of 143 reads, variant allele frequency

0.98, Fig. 3B).

We then analyzed signaling in response to interferon alpha, beta and gamma in these two cell

lines. M368 with the *JAK2* loss of function mutation maintained signaling in response to

interferon alpha and beta, but did not respond to interferon gamma (Fig. 3C), which resulted in

intact ability to upregulate PD-L1 when exposed to interferon alpha and beta, but not with

interferon gamma (Fig. 3C and Supplementary Fig. 9A and 9B). M395 with the *JAK1* loss of

function mutation did not respond to downstream signaling to either interferon alpha, beta or

gamma (Fig. 3D), and equally did not upregulate PD-L1 in response to either of these cytokines

(Fig. 3D and Supplementary Fig. 9A and 9B). We were able to retrieve the tumor from which the

cell line M395 had been established, and this tumor had absence of CD8 infiltration similar to

the finding of patient #15 with a JAK1 loss of function mutation not responding to anti-PD-1

therapy (Supplementary Fig. 11). Taken together, these data are consistent with the knowledge

8

that JAK1 (disabled in M395) is required to propagate signaling downstream of the interferon alpha/beta and gamma receptors, while JAK2 (disabled in M368) is required for signaling downstream only from the interferon gamma receptor (22-24).

To assess a causal relationship between loss of adaptive PD-L1 expression and loss-of-function *JAK* mutations, we transduced the M395 and M431 cell lines with a lentivirus vector expressing *JAK1* wild-type (Supplementary Fig. 12A-C). Reintroducing the JAK1 wild-type protein corrected the interferon gamma-induced PD-L1 expression for M395, with a 4-fold increase in PD-L1 surface expression after interferon gamma exposure (Fig. 3E). For M431, the magnitude of change in PD-L1 expression after 18-hour interferon gamma exposure for M431 was modest after reintroducing the JAK1 wild-type protein (approximately 2-fold, compared to a 1.5 fold in the untransduced cell line) (Fig. 3F). However, the difference between untransduced and JAK1 wild-type transduced M431 was more distinct when observed over a longer time course (Fig. 3G and 3H).

JAK Loss of Function Mutations in Primary Resistance to PD-1 Blockade in Patients with Metastatic Colon Carcinoma

To determine whether JAK1/2 loss of function mutations are present and relate to response to PD-1 blockade therapy in another cancer histology, we analyzed whole exome sequencing data from 16 biopsies of patients with colon cancer, many with a high mutational load resultant from mismatch-repair deficiency (6). One of the biopsies of a rare patient with high mutational load with neither an objective response nor disease control with anti-PD-1 had a homozygous *JAK1 W690** nonsense loss-of-function mutation, expected to truncate the protein within the first kinase domain, and an accompanying loss of heterozygosity at the *JAK1* locus (Fig. 4A-D). No mutations in antigen presentation machinery were detected in this sample (Supplementary Fig. 13). Although we observed other interferon-pathway and antigen presentation mutations in the

9

high mutational load patients with a response to therapy in this cohort, they appeared to be heterozygous by allele frequency (adjusted VAF < 0.6) after adjustment for stromal content. Most were splice site mutations or frameshift insertions/deletions unlikely to create a dominant-negative effect. Several samples bore two mutations in *JAK1/2* or *B2M*, but either retained at least one wild-type copy (subjects #4 and #5), were too far apart to determine cis vs trans status (subject #6), or were of uncertain significance (subject #1, both near c-terminus).

Frequency of *JAK* Loss of Function Mutations in Cell Lines of Multiple Histologies

We then analyzed data from the Cancer Cell Line Encyclopedia (CCLE) from cBioPortal to determine the frequency of homozygous putative loss of function mutations in *JAK1/2* in 905 cancer cell lines (25). For this analysis, we considered a homozygous mutation when the variant allele frequency was 0.8 or greater, as previously described (26). Approximately 0.7 % of cell lines have loss of function mutations that may predict lack of response to interferons (Fig. 5A and 5B). The highest frequency of mutations was in endometrial cancers, as described previously (26). None of these cell lines had POLE or POLD1 mutations, but microsatellite instability and DNA damage gene mutations were present in the *JAK1/2* mutant cell lines (Supplementary Fig. 14). The frequency of *JAK1/2* mutations across all cancers suggests that there is a fitness gain with loss of interferon responsiveness.

JAK1/2 Loss of Function Alterations in The Cancer Genome Atlas (TCGA)

Analysis of WES, RNASeq and reverse-phase protein array (RPPA) data from tissue specimens from 472 patients in the TCGA Skin Cutaneous Melanoma dataset revealed that 6% (28 of 472) and 11% (50 of 472) harbored alterations in *JAK1* and *JAK2*, respectively. These include loss of function alterations in either *JAK1 or JAK2* that would putatively diminish JAK1 or JAK2 signaling (homodeletions, truncating mutations or gene or protein downregulation).

10

There was no survival difference in patients in the TCGA Skin Cutaneous Melanoma dataset harboring any *JAK1* or *JAK2* alteration (Fig. 6A). However, when only considering loss of function *JAK1 or JAK2* alterations *(*homodeletions, truncating mutations or gene or protein downregulation), patients with tumors that had *JAK1* or *JAK2* alterations had significantly decreased overall survival (p = 0.009, log-rank test). When considered separately, the eight patients with truncating mutations in *JAK1* or *JAK2* and the 18 patients with *JAK1* or *JAK2* gene or protein downregulation also had significantly decreased overall survival (p=.016 and p<.001, respectively).

To assess the relevance of these findings in a broader set of malignancies, we examined the frequency of *JAK1* and *JAK2* alterations and their association with clinical outcome in TCGA datasets for four common malignancies (breast invasive carcinoma, prostate adenocarcinoma, lung adenocarcinoma, and colorectal adenocarcinoma). Similar to findings in melanoma, alterations in *JAK1* were found in 6%, 8%, 10% and 10% of patients with breast invasive carcinoma, prostate adenocarcinoma, lung adenocarcinoma and colorectal adenocarcinoma. Likewise, alterations in *JAK2* were found in 12%, 7%, 12% and 5% of these respective malignancies.

Consistent with our findings in melanoma, *JAK 1* or *JAK2* alterations as a whole were not associated with a difference in survival in any of the four additional TCGA datasets. However, for patients with breast invasive carcinoma harboring truncating mutations, there was an association with decreased survival (p=.006, log-rank test, Fig. 6B). Likewise, patients with prostate adenocarcinoma harboring truncating mutations had worse overall survival (p=.009, log-rank test, Fig. 6C), with a similar trend noted in patients harboring any loss of function *JAK1 or JAK2* alteration (p=.083, Fig. 6C). We did not observe differences in survival in patients with lung adenocarcinoma or colorectal adenocarcinoma harboring *JAK1* or *JAK2* loss of function

11

alterations, either when considered separately or as a whole (Supplementary Fig. 15A and 15B).

12

Discussion

For this work we hypothesized that if cancer cells evolved to disable inducible PD-L1 expression upon interferon exposure due to selective immune pressure as demonstrated in preclinical models of cancer immune-editing (15, 16), then it would be superfluous to attempt to treat these cases with anti-PD-1/L1 antibody therapy (Supplementary Fig. 16A and 16B). The premise of therapy with anti-PD-1 or anti-PD-L1 blocking antibodies is that T cells with specificity for cancer antigens recognize their target on cancer cells and produce interferon gamma. The cancer cell then finds a way to specifically protect itself from the T cell attack by reactively expressing PD-L1 upon interferon gamma signaling. This reactive process is termed adaptive immune resistance, and it requires signaling through the interferon gamma receptor (12). By understanding this process, then it is logical to anticipate that a genetically acquired insensitivity to interferon gamma signaling could represent an immune resistance mechanism; these tumors would be expected to be incapable of up-regulating either antigen presenting machinery or PD-L1 even in the presence of a robust pre-existing repertoire of tumor-specific T cells. With a genetic mechanism of lack of interferon gamma signaling, a T cell response with interferon gamma production would not lead to reactive PD-L1 expression and therefore these would be cases that would be considered constitutively PD-L1 negative.

JAK kinases mediate signaling from many cytokine receptors, but the commonality between *JAK1* and *JAK2* homozygous loss of function mutations is that they are both required for signaling upon exposure to interferon gamma (27). Interferon gamma is a major cytokine produced by T cells upon recognizing their cognate antigen and it has multiple effects on target cells. In the setting of acquired resistance to PD-1 blockade therapy in patients who progressed while on continuous anti-PD-1 therapy, the tumor's insensitivity to interferon gamma provides a selective advantage for the relapsed cancer to grow as it no longer is sensitive to the anti-

13

proliferative effects of interferon gamma (14). In that setting, T cells continued to recognize cancer cells with *JAK1* or *JAK2* mutations despite the known role of interferon gamma signaling in upregulating a series of genes involved in the antigen presenting machinery. However, as the baseline expression of MHC class I, proteasome subunits and TAP transporters is unchanged, then tumor antigen presentation to T cells was not impaired (14).

In primary resistance to checkpoint blockade therapy with the anti-CTLA-4 antibody ipilimumab, there is a higher frequency of mutations in the several molecules involved in the interferon signaling pathway (18). It is hypothesized that cancer cells lacking interferon receptor signaling would have a selective advantage because they evade T cells activated by CTLA-4 blockade, in particular through decreased antigen presentation and resistance to the anti-proliferative effects of interferons. The same processes may have an important role in the lack of response to anti-PD-1 therapy in the cancers with *JAK1/2* loss of function mutations in our series, as antitumor T cells would be anticipated to have lower ability to recognize and kill cancer cells. Loss of function mutations in *JAK1/2* would likewise prevent the antitumor activity of any immunotherapy that results in the activation of T cells to attack cancer cells. But in the setting of anti-PD-1/L1 therapy, it has the additional important effect of preventing PD-L1 expression upon interferon gamma exposure, thereby making it futile to pharmacologically inhibit the PD-L1/PD-1 interaction.

As the interferon gamma receptor pathway downstream of JAK1/2 controls the expression of chemokines with potent chemoattractant effect on T cells, such as CXCL9, CXCL10 and CXCL11 (28), it is possible that an important effect of *JAK1/2* loss may result in lack of T cell infiltrates. Indeed, in both the patient in the melanoma series with a *JAK1* loss of function and the biopsy from which we had derived a melanoma cell line with a *JAK1* mutation were completely devoid of T cell infiltrates. As pre-existing T cells in the tumor are a requisite for

14

response to anti-PD-1 therapy (11), then a *JAK1/2* mutation may result in lack of response not only because PD-L1 cannot be reactively expressed but also because the cancer fails to attract T cells due to lack of chemokine production.

Beyond a genetic mutation that prevented expression of *JAK1/2*, it is also possible that epigenetic silencing of *JAKs* could result in lack of response to interferon gamma, as previously reported for the LNCAP cell line (29). In this case, loss of JAK1/2 expression could then be corrected with exposure to a demethylating agent. This evidence suggests that the frequency of loss-of-function in *JAK1/2* may be higher than can be estimated by exome sequencing analyses as it could occur epigenetically, and in these cases it would provide an option for pharmacological intervention.

In conclusion, we propose that *JAK1/2* mutations that lead to loss of interferon gamma signaling and prevent adaptive PD-L1 expression upon interferon gamma exposure represent an immunoediting process that define patients with cancer that would not be good candidates for PD-1 blockade therapy. This mechanism would add to other multiple explanations that may lead to primary resistance to PD-1 blockade therapy, including a tumor that lacks antigens that can be a target for a T cell response, the presence of immune suppressive factors in the tumor microenviroment that exclude T cells in tumors or that lead to alteration of T cell function, presence of immune suppressive cells such as T regulatory or myeloid-derived suppressor cells, or cancers that have specific genetic signaling or transcriptomes that are not permissive to T cell infiltrates (20, 30, 31). The recognition that *JAK1/2* loss of function mutations would lead to lack of response to PD-1 blockade therapy could be incorporated in oncogenic sequencing panels used to select patients for precision cancer treatments.

Methods

Tumor samples Tumor biopsies were obtained from a subset of patients enrolled in a phase 1 expansion clinical trial with pembrolizumab after signing a written informed consent (32). Patients were selected for this analysis by having adequate tumor biopsy samples and clinical follow up. Baseline biopsies of metastatic tumors were obtained within 30 days of starting on treatment, except for one in a patient with an eventual complete response (Fig 3B subject #4) collected 84 days on treatment. Samples were immediately fixed in formalin followed by paraffin embedding, and when there was additional sterile piece of the tumor processed for snap-freezing in liquid nitrogen and to establish a cell line as previously described (33-35). Tumor biopsy and peripheral blood cell collection and analyses were approved by UCLA IRBs 11-001918 and 11-003066.

Treatment and response assessment. Patients received single agent pembrolizumab intravenously in one of three dosing regimens: 2 mg/kg every 3 weeks (2Q3W), 10 mg/kg every 3 weeks (10Q3W), or 10 mg/kg every 2 weeks (10Q2W) (32). Tumor responses to pembrolizumab were evaluated at 12 weeks after the first infusion (confirmed at 16 weeks), and every 12 weeks thereafter. The Response Evaluation Criteria in Solid Tumors (RECIST) version 1.1 was used to define objective clinical responses. The protocol allowed to proceed beyond initial progression at the restaging scans at 12 weeks and have repeated imaging scans 4 weeks later following the immune-related response criteria (irRC) (36).

Immunohistochemical (IHC) staining. For CD8 density, five out of the 11 cases were re-analyzed blindly from IHC samples already used in our prior work (11), and other 6 cases were newly stained cases also analyzed blindly. Slides were stained with hematoxylin and eosin, S100, CD8, CD68, PD-1 and PD-L1 at the UCLA Anatomic Pathology IHC Laboratory.

16

Immunostaining was performed on Leica Bond III autostainers using Leica Bond ancillary reagents and REFINE polymer DAB detection system as previously described (11). Cell density (cells/mm^2) in the invasive margin or intratumoral area was calculated using the Indica Labs Halo platform as previously described (11).

Cell lines, cell culture and conditions. Patient-derived melanoma cell lines were generated as reported previously and characterized for their oncogenic mutational status (33-35). Each melanoma cell line was thawed and maintained in RPMI-1640 medium supplemented with 10 % fetal bovine serum, 100 units/ml penicillin and 100 μg/ml streptomycin at 37°C in a humidified atmosphere of 5% CO_2. Cells were subject to experimental conditions after reaching two passages from thawing. Cell lines were periodically authenticated using GenePrint® 10 System (Promega, Madison, WI), and were matched with the earliest passage cell lines. Selected melanoma cell lines were subjected to mycoplasma tests periodically (every 2-3 months) by MycoAlert Mycoplasma detection Kit (Lonza, Walkersville, MD).

Surface flow cytometry analysis for PD-L1 and MHC class I. Melanoma cells were seeded into 6 well plates on day 1, ranging from 420,000 to 485,000 depending on their doubling time, targeting 70-80% of confluence at the time of trypsinization after 18 hours of exposure to interferons. For 48 hours exposure, 225,000 to 280,000 cells were seeded, and 185,000 to 200,000 cells were seeded for 72 hours exposure. After trypsinization, cells were incubated at 37°C for 2 hours with media containing different concentrations of interferons. Concentrations of each interferon were determined after optimization process (dose response curves were generated with representative cell lines as shown in Supplementary Fig. 5B-D). After 2 hours of incubation, the media was removed by centrifugation and cells were re-suspended with 100% FBS, stained with APC anti-PD-L1 antibody on ice for 20 minutes. The staining was halted by washing with 3 ml of phosphate buffered saline (PBS), which was removed by centrifugation at

17

500g for 4 minutes. The cells were re-suspended with 300 µl of PBS, 7-AAD for dead cell discrimination was added to samples prior to data acquisition by LSRII. The data were analyzed by Flowjo software (Version 10.0.8r1, Tree Star Inc., Asland, OR). Experiments were performed at least twice for each cell line; some cell lines with high assay variability were analyzed three times.

Phosphoflow signaling analyses. Cells were seeded into two 6 well plates for each cell line for single phospho-proteomics study. After 30 minute or 18 hour exposure to interferon alpha, beta or gamma, cells were trypsinized and re-suspended with 1 ml of PBS per 1-3 million cells, stained with live/dead agent at room temperature in the dark for 30 minutes. Cells were then fixed with paraformaldehyde at room temperature for 10 minutes in the dark and permeabilized by methanol and stained with pSTAT1. Cells were incubated at room temperature in the dark for 30 minutes and washed with phospho-flow cytometry buffer and re-suspended with 300 to 500 µl of the same buffer and analyzed with a LSRII. The FCS files obtained by LRSII were analyzed using the online flow cytometry program (cytobank) (37). The raw FCS files were de-convoluted into four different conditions, three of which were exposed to interferon alpha, beta and gamma and compared to an untreated condition at each time point. Data represented as Arcsinh ratio, which is one of transformed ratio of cytometry data (inverse hyperbolic sine) analyses, each data point was compared to its control. [Value = arcsinh((x - control) / scale_argument)].

Western blot analyses. Selected melanoma cells were maintained in 10 cm cell culture dishes and exposed to interferon alpha, beta or gamma (same concentrations as above) for 30 minutes or 18 hours. Western blotting was performed as described previously (38). Primary antibodies included pJak1 (Tyr1022/1023), pJAK2 (Tyr221), pSTAT1 (Tyr701), pSTAT3 (Tyr705), pSTAT5 (Tyr695) and their total proteins; PIAS1, IRF-1, SOCS1 and GAPDH (all from Cell Signaling

18

Technology, Danvers, MA). Immuno-reactivity was revealed with an ECL-Plus kit (Amersham Biosciences Co, Piscataway, NJ), using the ChemiDoc MP system (Bio-rad Laboratories, Hercules, CA).

Lentiviral vector production and gene transfer. Lentivirus production was performed by transient co-transfection of 293T cells (ATCC, Rockville, MD). The lentiviral vectors pLenti-C-mGFP and pLenti-C-JAK1-mGFP were purchased from Origen (Cat # RC213878L2, Rockville, MD). In brief, T175 tissue culture flasks, coated with poly-L-lysine (Sigma Aldrich, St. Louis, MO) containing 6×10^6 293T cells were used for each transfection. The constructs required for the packaging of third generation self-inactivating lentiviral vectors pLenti-C-mGFP and pLenti-C-JAK1-mGFP (60 µg), pMDLGg/p (39 µg), pRSV–REV (15 µg), and pMD.G (21 µg) were dissolved in water in a total volume of 2.7 ml. A total of 300 µl of 2.5M $CaCl_2$ (Sigma Aldrich) was added to the DNA mixture. A total of 2.8 ml of the DNA/CaCl2 mix was added dropwise to 2.8 ml of 2X HBS buffer, pH 7.12 (280 nM NaCl, 1.5 mM Na_2HPO_4, 100mM HEPES). The DNA/$CaPO_4$ suspension was added to each flask and incubated in a 5% CO2 incubator at 37°C overnight. The next morning, the medium was discarded, the cells were washed, and 15 ml DMEM medium with 10% fetal bovine serum containing 20 mM HEPES (Invitrogen, Carlsbad, CA) and 10 mM sodium butyrate (Sigma Aldrich) was added and the flask incubated at 37°C for 8 to 12 hours. After that, the cells were washed once and 10 ml fresh DMEM medium with 20 mM Hepes was added onto the 293T cells, which were further incubated in a 5% CO_2 incubator at 37°C for 12 hours. The medium supernatants were then collected, filtered through 0.2 µM filters and cryopreserved at minus 80°C. Virus supernatant was added at different concentrations into six-well plates containing 5×10^5 cells per well. Protamine sulphate (Sigma Aldrich) was added at a final concentration of 5 µg/ml and the transduction plates were incubated at 37°C in 5% CO_2 overnight.

Whole exome sequencing. Exon capture and library preparation were performed at the UCLA Clinical Microarray Core using the Roche Nimblegen SeqCap EZ Human Exome Library v3.0 targeting 65 Mb of genome. 2x100bp paired-end sequencing was carried out on the HiSeq 2000 platform (Illumina, San Diego, CA) and sequences were aligned to the UCSC hg19 reference using BWA-mem (v0.7.9). Sequencing for tumors was performed to a target depth of 150X (Actual Min. 91X, Max. 162X, Mean. 130X). Pre-processing followed the Genome Analysis Toolkit (GATK) Best Practices Workflow v3, including duplicate removal (PicardTools), indel realignment, and base quality score recalibration.

Somatic mutations were called by comparison to sequencing of matched normals for the PD1-treated whole-tumor patient samples. Methods were modified from reference (39); specifically the substitution the GATK-HaplotypeCaller (HC, v3.3) for the UnifiedGenotyper. gVCF outputs from GATK-HC for all 23 tumor/normal exomes, and cell lines M395 and M431, were jointly genotyped and submitted for variant quality score recalibration. Somatic variants were determined using one-sided Fisher's exact test (P value cut-off ≤ 0.01) between tumor/normal pairs with depth >10 reads. Only high-confidence mutations were retained for final consideration, defined as those identified by at least two out of three programs (MuTect (v1.1.7) (40), Varscan2 Somatic (v2.3.6) (41), and the GATK-HC) for SNVs, and those called by both Varscan2 and the GATK-HC for insertions/deletions. Variants were annotated by Oncotator (42), with non-synonymous mutations for mutational load being those classified as Nonsense, Missense, Splice_Site, or Nonstop Mutations, as well as Frame_Shift, In_Frame_, or Start_Codon altering insertions/deletions. Adjusted variant allele frequency was calculated according to the following equation:.

$VAF adjusted = n_{mut}/CN_t = VAF*[1+(2*Stromal\ Fraction)/(Tumor\ Fraction*Local\ Copy\ Number)]$

This is an algebraic rearrangement of the equation used in the clonal architecture analysis from McGranaham et. al (43) to calculate the fraction of mutated chromosomal copies while adjusting

20

for the diluting contribution of stromal chromosomal copies. Local tumor Copy Number (CN_t,) Tumor Fraction (purity, or p) and Stromal Fraction (1-p) were produced by Sequenza (44), which uses both depth-ratio and SNP minor B-allele frequencies to estimate tumor ploidy, percent tumor content and perform allele-specific copy number variation analysis.

PDJ amplification was considered tumor/normal depth ratio >= 2 standard deviations above length-weighted genome average. BAM files for the 16 colorectal cases were previously mapped to hg18 and sequencing and analysis were performed at PGDx (Personal Genome Diagnostics, Baltimore, MD). After pre-processing and somatic variant calling, positions were remapped to hg19 using the Ensembl Assembly Converter before annotation.

M431 and M395 were compared to matched normal samples, the other 47 cell lines lacked a paired normal sample. For detection of potential JAK1 or JAK2 mutations, variants were detected using the Haplotype Caller, and noted for membership in dbSNP 146 and allele frequency from the 1000 Genomes project, and confirmed by visual inspection with the Integrated Genomics Viewer (IGV).

RT-PCR (reverse transcription-polymerase chain reaction). Forward 5'-AACCTTCTCACCAGGATGCG-3', reverse 5'-CTCAGCACGTACATCCCCTC-3' primers were designed to perform RT-PCR (700 base pair of target PCR product to cover P429 region of JAK1 protein) on M431 cell line. Total RNA was extracted by *mir*Vana™ miRNA Isolation Kit, with phenols as per manufacturer's protocol (Thermo Fischer Scientific, Whiltham, MA). RT-PCR was performed by utilizing ThermoScript™ RT-PCR Systems (Thermo Fisher Scientific, cat# 11146-057). PCR product was subject to Sanger sequencing at UCLA core facility.

TCGA Analysis. To determine the relevance of *JAK1* and *JAK2* alterations in a broader set of patients, we queried the TCGA skin cutaneous melanoma provisional dataset for the frequency of genetic and expression alterations in *JAK1* and *JAK2*. We then extended our query to the breast invasive carcinoma, prostate adenocarcinoma, lung adenocarcinoma and colorectal adenocarcinoma provisional TCGA datasets. We then examined the association of various *JAK1* and *JAK2* alterations with overall survival for each dataset. The results are based upon data generated by the TCGA Research Network and made available through the NCI Genomic Data Commons and cBioPortal (45, 46).

The Mutation Annotation Format (MAF) files containing *JAK1* and *JAK2* mutations in the TCGA datasets were obtained from Genomic Data Commons. In addition, mutations, putative copy-number alterations, mRNA expression, protein expression and survival data were obtained using the cBioPortal resource. The putative copy-number alterations (homodeletion events, in particular) available in cBioPortal were obtained from the TCGA datasets using Genomic Identification of Significant Targets in Cancer (GISTIC) (47). The mRNA expression data available in cBioPortal were obtained from the TCGA datasets using RNA Seq (RNA Seq V2 RSEM). Up and downregulation of *JAK1* and *JAK2* mRNA expression were determined using an mRNA z-Score cutoff of 2.0. Protein expression data available in cBioPortal was obtained from the TCGA dataset using RPPA, with a z-score threshold of 2.0.

Mutation data between the MAF files and data from cBioPortal were combined. Genetic and expression alterations were characterized in one of six categories: amplifications, homodeletions, single nucleotide polymorphisms, truncating mutations (stop codons and frame-shift insertions and deletions), mRNA or protein downregulation, and mRNA or protein upregulation. The frequency of *JAK1* and *JAK2*alterations were determined using combined data from the *.MAF file and cBioPortal. Kaplan-Meier survival curves were generated in R,

22

using the 'survminer' package and the 'ggsurvplot' function. Survival of overall survival was determined using log-rank analysis.

Statistical analysis. Statistical comparisons were performed by the unpaired two-tailed Student's *t* test, (GraphPad Prism, version 6.0 for windows). Mutational load was compared by unpaired two-sided Mann-Whitney test. R programming was utilized to generate arrow graphs of PD-L1/MHC class I expression upon interferon exposures and the CCLE JAK1/2 mutation frequency graph.

23

Author Contributions. B.C-A. and A.R. supervised the project and developed the concepts. D.S.S., J.M.Z., H.E.O., A.G.D., B.C-A. and A.R. designed the experiments. D.S.S., B.C-A. and A.R. interpreted the data. D.S.S. and B.C-A. performed the flow cytometry studies. D.S.S., H.E.O. and A.G.D. performed interferon signaling studies. D.S.S. and H.E.O performed lentiviral transduction. A.G.D., S.S., D.Y.T and G.A.R. generated JAK1 knockouts. B.B-M. established cell lines. S.H-L., I.P.S. and P.C.T. performed the immunohistochemistry analyses. J.M.Z., A.K., C.S.G., N.P., W.H., D.T.L., D.M.P., L.A.D, T.G.G., and R.S.L. performed genomic analyses. B.C., G.C., E.S., P.C.T., R.S.L. and A.R. clinically evaluated patients. D.S.S. and A.R. wrote the manuscript. All authors contributed to the manuscript and approved the final version.

24

References:

1.   Herbst RS, Soria JC, Kowanetz M, Fine GD, Hamid O, Gordon MS, et al. Predictive correlates of response to the anti-PD-L1 antibody MPDL3280A in cancer patients. Nature. 2014;515:563-7.

2.   Powles T, Eder JP, Fine GD, Braiteh FS, Loriot Y, Cruz C, et al. MPDL3280A (anti-PD-L1) treatment leads to clinical activity in metastatic bladder cancer. Nature. 2014;515:558-62.

3.   Robert C, Long GV, Brady B, Dutriaux C, Maio M, Mortier L, et al. Nivolumab in previously untreated melanoma without BRAF mutation. N Engl J Med. 2015;372:320-30.

4.   Ansell SM, Lesokhin AM, Borrello I, Halwani A, Scott EC, Gutierrez M, et al. PD-1 blockade with nivolumab in relapsed or refractory Hodgkin's lymphoma. N Engl J Med. 2015;372:311-9.

5.   Robert C, Schachter J, Long GV, Arance A, Grob JJ, Mortier L, et al. Pembrolizumab versus Ipilimumab in Advanced Melanoma. N Engl J Med. 2015;372:2521-32.

6.   Le DT, Uram JN, Wang H, Bartlett BR, Kemberling H, Eyring AD, et al. PD-1 Blockade in Tumors with Mismatch-Repair Deficiency. N Engl J Med. 2015;372:2509-20.

7.   Garon EB, Rizvi NA, Hui R, Leighl N, Balmanoukian AS, Eder JP, et al. Pembrolizumab for the treatment of non-small-cell lung cancer. N Engl J Med. 2015;372:2018-28.

8.   Nghiem PT, Bhatia S, Lipson EJ, Kudchadkar RR, Miller NJ, Annamalai L, et al. PD-1 Blockade with Pembrolizumab in Advanced Merkel-Cell Carcinoma. N Engl J Med. 2016;374:2542-52.

9.   Pardoll DM. The blockade of immune checkpoints in cancer immunotherapy. Nature reviews Cancer. 2012;12:252-64.

10.   Taube JM, Anders RA, Young GD, Xu H, Sharma R, McMiller TL, et al. Colocalization of inflammatory response with B7-h1 expression in human melanocytic lesions supports an adaptive resistance mechanism of immune escape. Sci Transl Med. 2012;4:127ra37.

11.   Tumeh PC, Harview CL, Yearley JH, Shintaku IP, Taylor EJ, Robert L, et al. PD-1 blockade induces responses by inhibiting adaptive immune resistance. Nature. 2014;515:568-71.

12.   Ribas A. Adaptive Immune Resistance: How Cancer Protects from Immune Attack. Cancer Discov. 2015;5:915-9.

13.   Bach EA, Aguet M, Schreiber RD. The IFN gamma receptor: a paradigm for cytokine receptor signaling. Annu Rev Immunol. 1997;15:563-91.

14.   Zaretsky JM, Garcia-Diaz A, Shin DS, Escuin-Ordinas H, Hugo W, Hu-Lieskovan S, et al. Mutations Associated with Acquired Resistance to PD-1 Blockade in Melanoma. N Engl J Med. 2016;375:819-29.

15.   Dunn GP, Bruce AT, Ikeda H, Old LJ, Schreiber RD. Cancer immunoediting: from immunosurveillance to tumor escape. Nat Immunol. 2002;3:991-8.

16.   Kaplan DH, Shankaran V, Dighe AS, Stockert E, Aguet M, Old LJ, et al. Demonstration of an interferon gamma-dependent tumor surveillance system in immunocompetent mice. Proc Natl Acad Sci U S A. 1998;95:7556-61.

17.   Mazzolini G, Narvaiza I, Martinez-Cruz LA, Arina A, Barajas M, Galofre JC, et al. Pancreatic cancer escape variants that evade immunogene therapy through loss of sensitivity to IFNgamma-induced apoptosis. Gene Ther. 2003;10:1067-78.

18.   Gao J, Shi LZ, Zhao H, Chen J, Xiong L, He Q, et al. Loss of IFN-gamma Pathway Genes in Tumor Cells as a Mechanism of Resistance to Anti-CTLA-4 Therapy. Cell. 2016;167:397-404 e9.

19.   Rizvi NA, Hellmann MD, Snyder A, Kvistborg P, Makarov V, Havel JJ, et al. Cancer immunology. Mutational landscape determines sensitivity to PD-1 blockade in non-small cell lung cancer. Science. 2015;348:124-8.

20.   Hugo W, Zaretsky JM, Sun L, Song C, Moreno BH, Hu-Lieskovan S, et al. Genomic and Transcriptomic Features of Response to Anti-PD-1 Therapy in Metastatic Melanoma. Cell. 2016;165:35-44.

21.   Rosenberg JE, Hoffman-Censits J, Powles T, van der Heijden MS, Balar AV, Necchi A, et al. Atezolizumab in patients with locally advanced and metastatic urothelial carcinoma who have progressed following treatment with platinum-based chemotherapy: a single-arm, multicentre, phase 2 trial. Lancet. 2016;387:1909-20.

22.   Rodig SJ, Meraz MA, White JM, Lampe PA, Riley JK, Arthur CD, et al. Disruption of the Jak1 gene demonstrates obligatory and nonredundant roles of the Jaks in cytokine-induced biologic responses. Cell. 1998;93:373-83.

23.   Muller M, Briscoe J, Laxton C, Guschin D, Ziemiecki A, Silvennoinen O, et al. The protein tyrosine kinase JAK1 complements defects in interferon-alpha/beta and -gamma signal transduction. Nature. 1993;366:129-35.

24.   Watling D, Guschin D, Muller M, Silvennoinen O, Witthuhn BA, Quelle FW, et al. Complementation by the protein tyrosine kinase JAK2 of a mutant cell line defective in the interferon-gamma signal transduction pathway. Nature. 1993;366:166-70.

25.   Barretina J, Caponigro G, Stransky N, Venkatesan K, Margolin AA, Kim S, et al. The Cancer Cell Line Encyclopedia enables predictive modelling of anticancer drug sensitivity. Nature. 2012;483:603-7.

26.   Ren Y, Zhang Y, Liu RZ, Fenstermacher DA, Wright KL, Teer JK, et al. JAK1 truncating mutations in gynecologic cancer define new role of cancer-associated protein tyrosine kinase aberrations. Scientific reports. 2013;3:3042.

27.   Platanias LC. Mechanisms of type-I- and type-II-interferon-mediated signalling. Nat Rev Immunol. 2005;5:375-86.

28.   Fish EN, Platanias LC. Interferon receptor signaling in malignancy: a network of cellular pathways defining biological outcomes. Mol Cancer Res. 2014;12:1691-703.

29.   Dunn GP, Sheehan KC, Old LJ, Schreiber RD. IFN unresponsiveness in LNCaP cells due to the lack of JAK1 gene expression. Cancer Res. 2005;65:3447-53.

30.   Spranger S, Bao R, Gajewski TF. Melanoma-intrinsic beta-catenin signalling prevents anti-tumour immunity. Nature. 2015;523:231-5.

31.   Sharma P, Allison JP. The future of immune checkpoint therapy. Science. 2015;348:56-61.

32.   Ribas A, Hamid O, Daud A, Hodi FS, Wolchok JD, Kefford R, et al. Association of Pembrolizumab With Tumor Response and Survival Among Patients With Advanced Melanoma. JAMA. 2016;315:1600-9.

33.   Nazarian R, Shi H, Wang Q, Kong X, Koya RC, Lee H, et al. Melanomas acquire resistance to B-RAF(V600E) inhibition by RTK or N-RAS upregulation. Nature. 2010;468:973-7.

34.   Atefi M, Avramis E, Lassen A, Wong DJ, Robert L, Foulad D, et al. Effects of MAPK and PI3K Pathways on PD-L1 Expression in Melanoma. Clin Cancer Res. 2014;20:3446-57.

35.   Wong DJ, Robert L, Atefi MS, Lassen A, Avarappatt G, Cerniglia M, et al. Antitumor activity of the ERK inhibitor SCH722984 against BRAF mutant, NRAS mutant and wild-type melanoma. Mol Cancer. 2014;13:194.

36.   Wolchok JD, Hoos A, O'Day S, Weber JS, Hamid O, Lebbe C, et al. Guidelines for the evaluation of immune therapy activity in solid tumors: immune-related response criteria. Clin Cancer Res. 2009;15:7412-20.

37.   Kotecha N, Krutzik PO, Irish JM. Web-based analysis and publication of flow cytometry experiments. Current protocols in cytometry / editorial board, J Paul Robinson, managing editor [et al]. 2010;Chapter 10:Unit10 7.

38.   Escuin-Ordinas H, Atefi M, Fu Y, Cass A, Ng C, Huang RR, et al. COX-2 inhibition prevents the appearance of cutaneous squamous cell carcinomas accelerated by BRAF inhibitors. Mol Oncol. 2014;8:250-60.

39.   Shi H, Hugo W, Kong X, Hong A, Koya RC, Moriceau G, et al. Acquired resistance and clonal evolution in melanoma during BRAF inhibitor therapy. Cancer Discov. 2014;4:80-93.

40.   Cibulskis K, Lawrence MS, Carter SL, Sivachenko A, Jaffe D, Sougnez C, et al. Sensitive detection of somatic point mutations in impure and heterogeneous cancer samples. Nat Biotechnol. 2013;31:213-9.

41.   Koboldt DC, Zhang Q, Larson DE, Shen D, McLellan MD, Lin L, et al. VarScan 2: somatic mutation and copy number alteration discovery in cancer by exome sequencing. Genome research. 2012;22:568-76.

42.   Ramos AH, Lichtenstein L, Gupta M, Lawrence MS, Pugh TJ, Saksena G, et al. Oncotator: cancer variant annotation tool. Human mutation. 2015;36:E2423-9.

43.   McGranahan N, Furness AJ, Rosenthal R, Ramskov S, Lyngaa R, Saini SK, et al. Clonal neoantigens elicit T cell immunoreactivity and sensitivity to immune checkpoint blockade. Science. 2016;351:1463-9.

44.   Favero F, Joshi T, Marquard AM, Birkbak NJ, Krzystanek M, Li Q, et al. Sequenza: allele-specific copy number and mutation profiles from tumor sequencing data. Ann Oncol. 2015;26:64-70.

45.   Cerami E, Gao J, Dogrusoz U, Gross BE, Sumer SO, Aksoy BA, et al. The cBio cancer genomics portal: an open platform for exploring multidimensional cancer genomics data. Cancer Discov. 2012;2:401-4.

46.   Gao J, Aksoy BA, Dogrusoz U, Dresdner G, Gross B, Sumer SO, et al. Integrative analysis of complex cancer genomics and clinical profiles using the cBioPortal. Sci Signal. 2013;6:pl1.

47.   Beroukhim R, Getz G, Nghiemphu L, Barretina J, Hsueh T, Linhart D, et al. Assessing the significance of chromosomal aberrations in cancer: methodology and application to glioma. Proc Natl Acad Sci U S A. 2007;104:20007-12.

Figure Legends

Figure 1. Mutational load and mutations in interferon signaling pathway among patients with advanced melanoma with or without response to anti-PD-1 blockade therapy. A) Total non-synonymous mutations per tumor from biopsies of patients with response (n=14) or without response (n=9) to anti-PD-1 per RECIST 1.1 criteria (median 503 versus 274, P = 0.27 by Mann-Whitney). Median and interquartile range are shown, with value for each individual tumor shown as dots. B-D) Each column corresponds to an individual case from panel A. B) Depiction of mutational load (bar graph) and mutations in interferon receptor pathway genes. The size of circles and adjacent labels represent the tumor variant allele frequency (VAF) after adjustment for stromal content. Color represents predicted functional effect. Green = missense; orange = nonsense. Red circle highlights amplified JAK1 mutation in one patient who did not respond to anti-PD-1 therapy. All the tumor sequences were compared to normal germline sequences. C) Heat map of the density of CD8 T cells in the invasive margin or intra-tumor compartment analyzed in baseline tumor biopsies by immunohistochemistry. D) Heat map of density of PD-L1 expression in available tissue samples. E) Genetic amplification of the chr9p24.1 (PD-L1, PD-L2 and JAK2 locus, termed the PDJ amplicon) was noted in one biopsy from a non-responding patient. Heat map represents average read depth ratio vs paired germline normal.

Figure 2. Altered interferon signaling with JAK1 loss of function mutation in M431 and interferon gamma-inducible PD-L1 expression by 48 melanoma cell lines. A) Mean fluorescent intensity of PD-L1 expression by flow cytometry upon interferon alpha, beta or gamma exposure over 18 hours in M431 (established from patient #15) compared with M438 (established from patient #8). B) Corresponding Western blot analyses for M431 upon interferon exposure for 30 minutes or 18 hours. C) Phosphorylated STAT1 (pSTAT1) flow cytometry for

28

M431 upon interferon exposure for 30 minutes or 18 hours (same color scale was in Fig. 2). The numbers in the heat map of pSTAT1 indicate the average Arcsinh ratio from two independent phospho-flow cytometry experiments. D) PD-L1 response to interferon gamma. Blue arrows represent average change from baseline upon interferon gamma exposure. Grey shades show the full range of measured values (n=2 or 3). Red stars indicate cell lines with no response and black stars indicate cell lines with poor response to interferons. Red: BRAF mutated; blue: NRAS mutated; green: BRAF and NRAS mutated; black: BRAF wild type, NRAS wild type.

Figure 3. Defects in interferon receptor signaling pathway with JAK homozygous loss of function mutations in M368 and M395. A and B) Exome sequencing data showing JAK2 D313 spice site mutation in exon 8 in M368 (A), and JAK1 D775N kinase domain mutation in exon 17 in M395 (B). Upper plot shows individual sequencing reads using the Integrated Genomics Viewer (IGV); lower plot shows position relative to kinase domains using the cBioPortal Mutation Mapper. C and D) For each cell line, cells were cultured with interferon alpha, interferon beta or interferon gamma for either 30 minutes or 18 hours, or with vehicle control (c, first column from the left in Western blots and phospho-flow data). Phosphorylated STAT1 (pSTAT1) detected by Western blotting (top panel) or phospho-flow cytometry data (bottom panel). The numbers in the heat map of pSTAT1 indicate the average Arcsinh ratio from two independent phospho-flow experiments. Blots represent two independent replicate experiments. E and F) PD-L1 expression after interferon exposure on M395 and M431 after JAK1 wild-type lentiviral transduction respectively. G and H) Time course PD-L1 expression for M431 and JAK1 wild type lentiviral vector transduced M431 respectively.

Figure 4. Mutational burden of somatic, protein-altering mutations per subject from whole exome sequencing for patients with advanced colon cancer who participated PD-1 blockade clinical trial. A) Similar to Fig. 1B, bar graph shows mutational load in individual

cases (fraction SNVs, blue; insertions, red; deletions, orange) divided by response to PD-1 blockade therapy. Bottom panel depicts mutations, insertions, or deletions in the interferon receptor pathway. Color represents predicted functional effect. The size of circles and adjacent labels correspond to tumor variant allele frequency (VAF) after adjusting for stromal content. Red circle highlights homozygous nonsense mutation in JAK1 from one of patient who did not respond to anti-PD-1 therapy. B) Sequencing reads of JAK1 mutation in non-responder subject # 12. C) Mutation observed in 51 reads out of 80, (VAF 0.64) which corresponds to a homozygous mutation (adjusted VAF 0.94) when adjusted for a tumor purity of 68%. D) Copy number profile reveals loss of heterozygosity across most of the genome, including chromosome 1/JAK1.

Figure 5. Analysis of JAK1 and JAK2 mutations in the Cancer Cell Line Encyclopedia database. A) Variant allele frequency (left axis, red and blue points) and percentage of tumors with mutations in JAK1 or JAK2 (right axis, grey bars) in CCLE database from the cBioPortal. B) Non-synonymous mutational burden was analyzed for individual cell lines (each dot represents cell line) and plotted for each histological type. *JAK1* or *JAK2* mutated cell lines were color coded (red: VAF>0.75 and blue: VAF<0.75).

Figure 6. Frequency of *JAK1* and *JAK2* alterations and their association with overall survival in TCGA datasets. Kaplan-Meier survival analysis of TCGA skin cutaneous melanoma (A), breast invasive carcinoma (B) and prostate adenocarcinoma (C) provisional datasets, comparing control patients (blue) and patients harboring specified alterations in *JAK1* and *JAK2* (red). Frequency and distribution of combined *JAK1* and *JAK2* alterations are shown within each set of Kaplan-Meier plots. Significance testing of overall survival was performed using log-rank analysis.
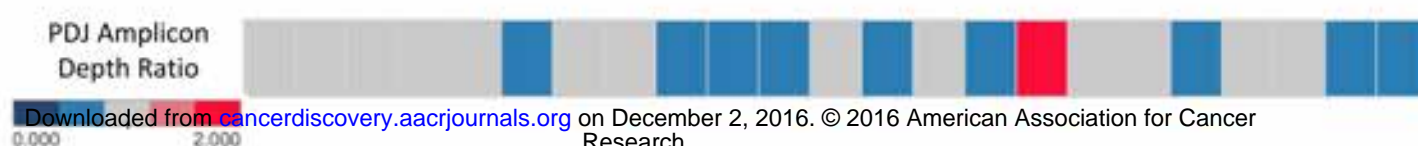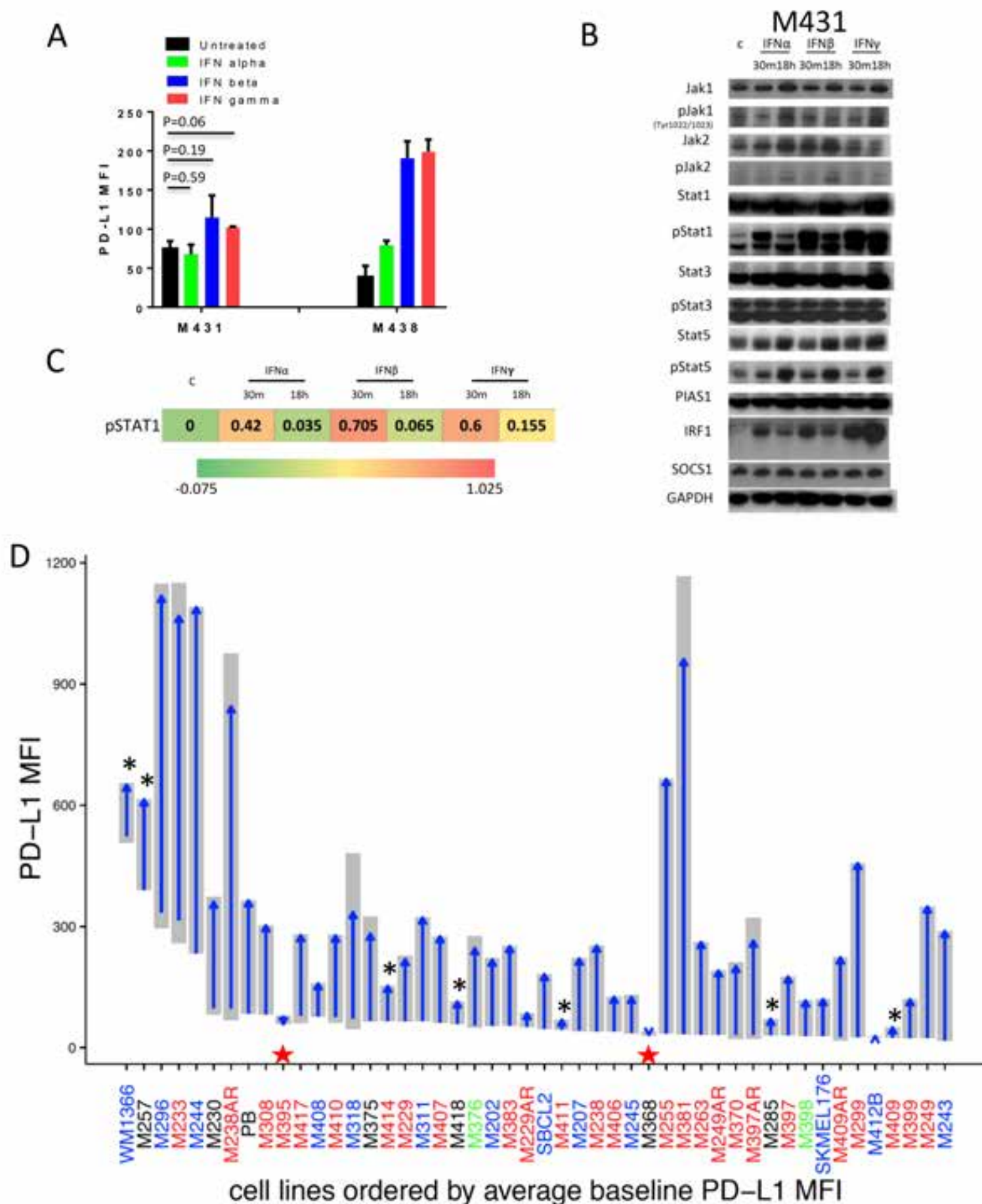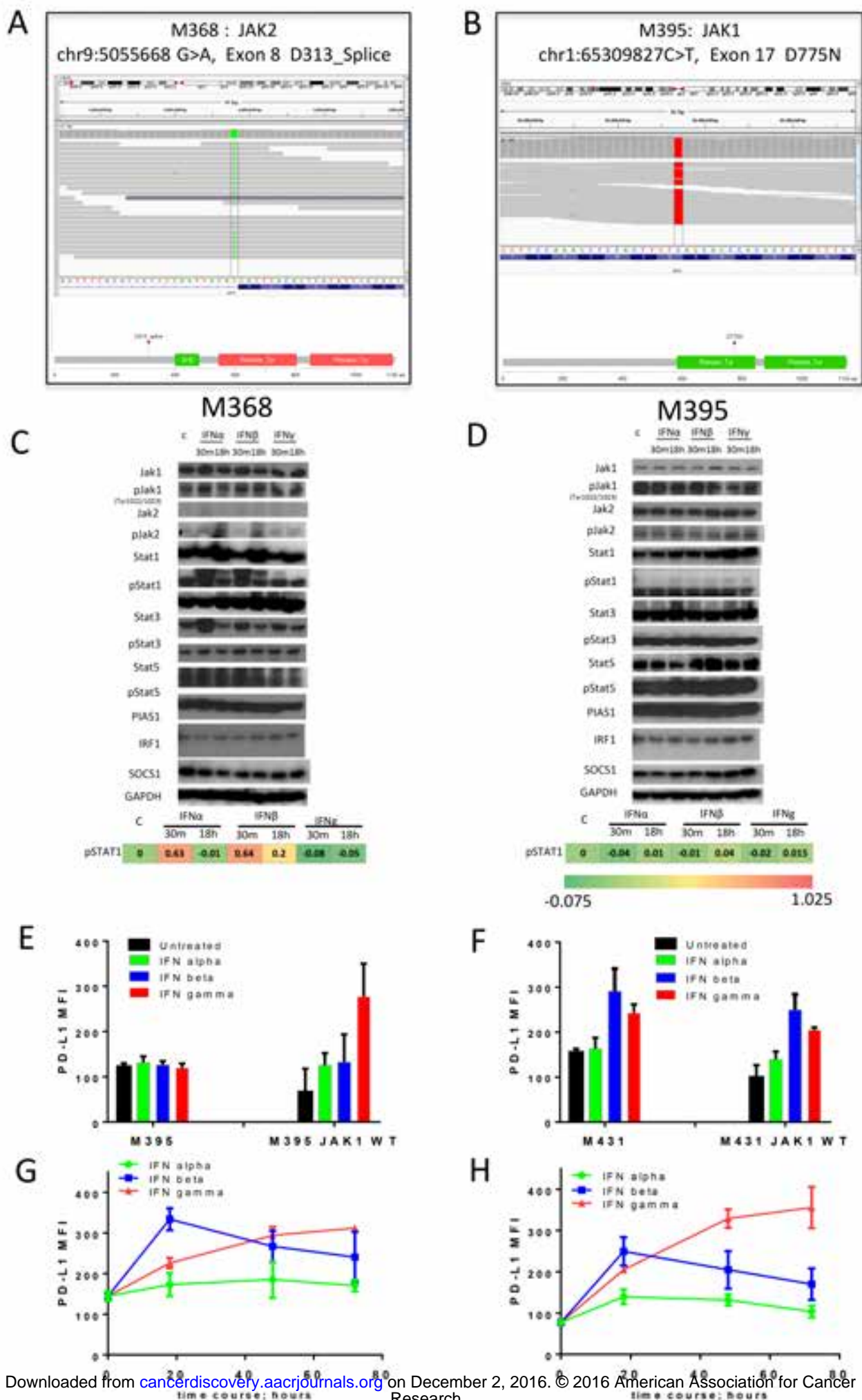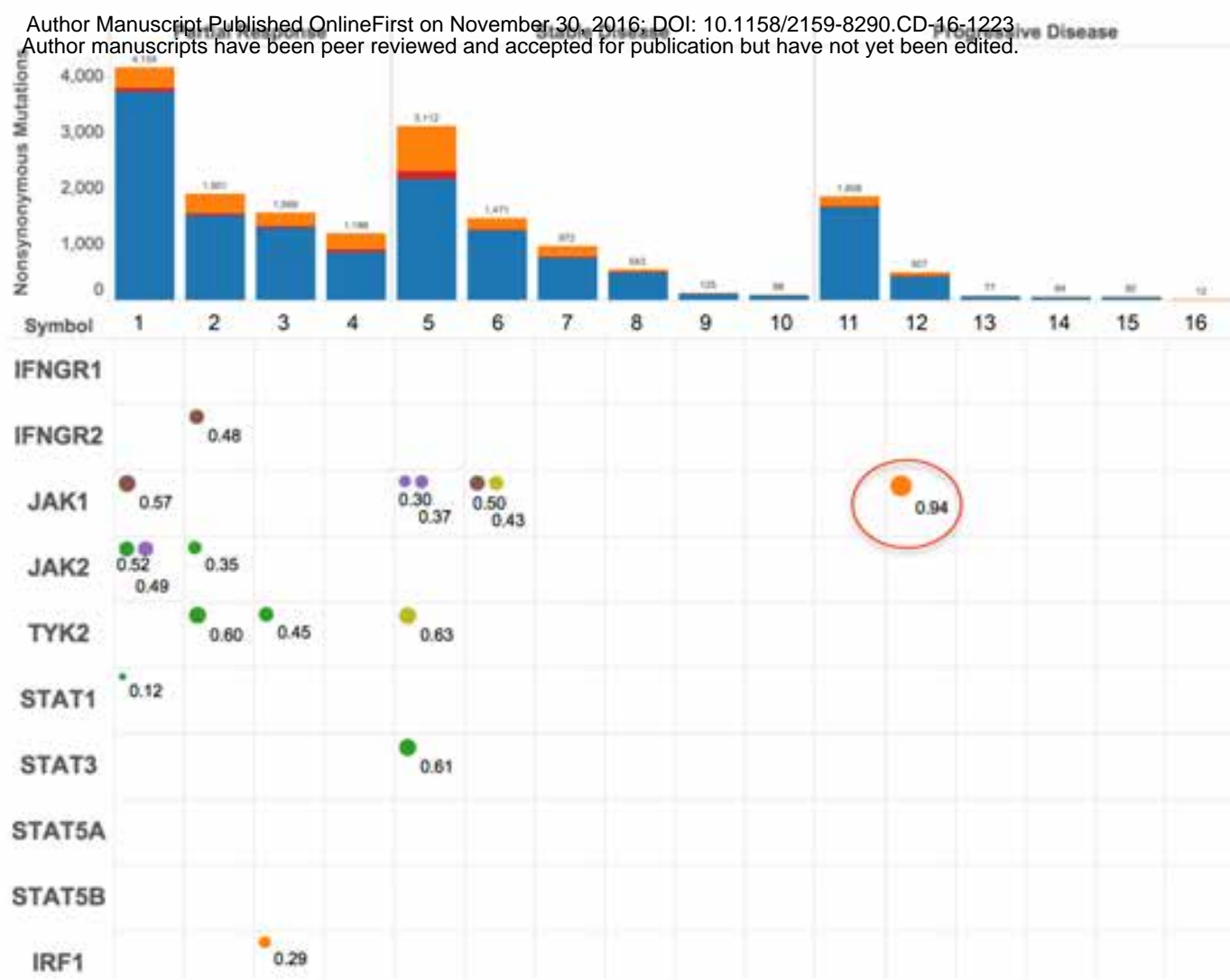
Figure 1

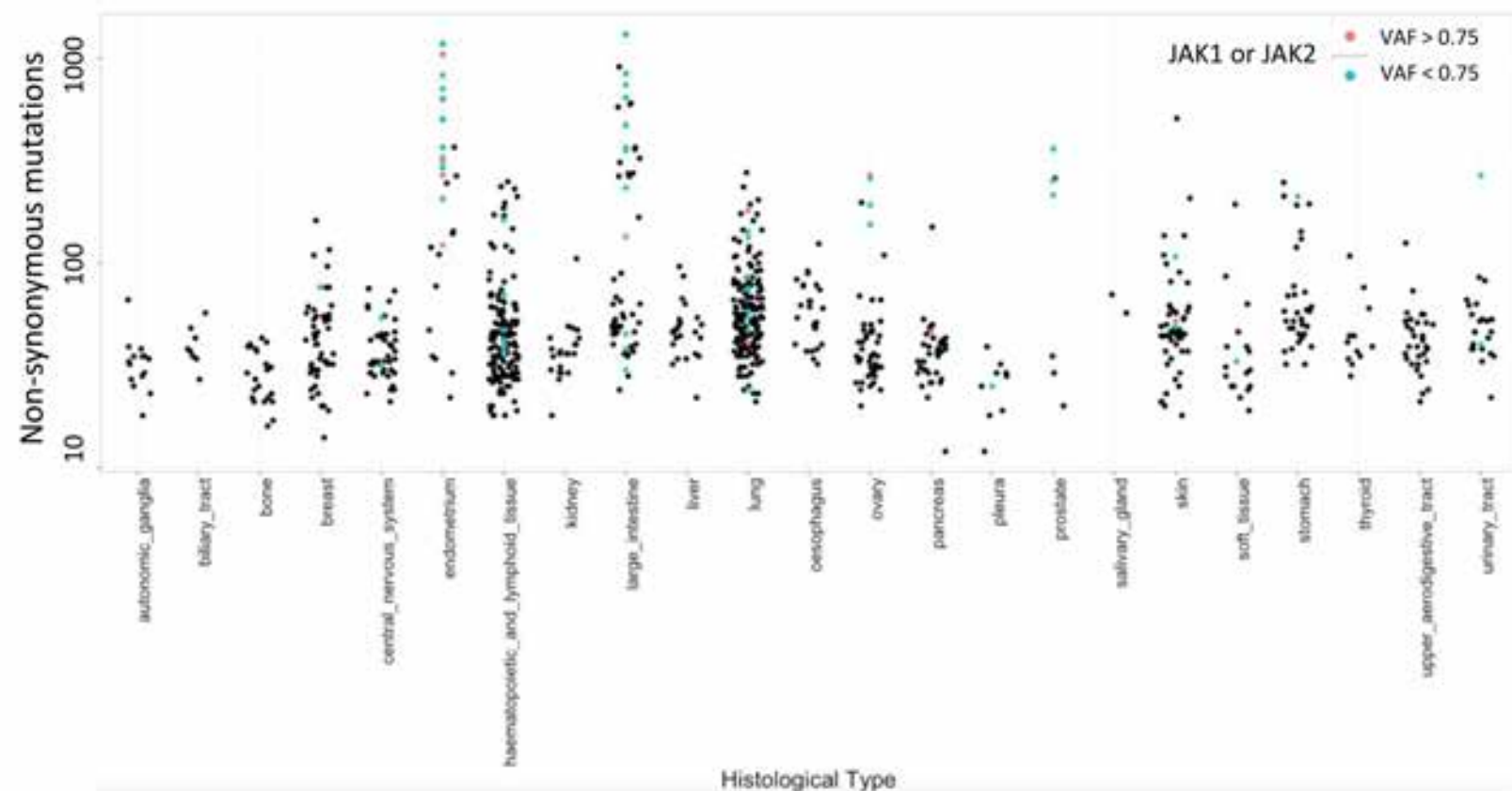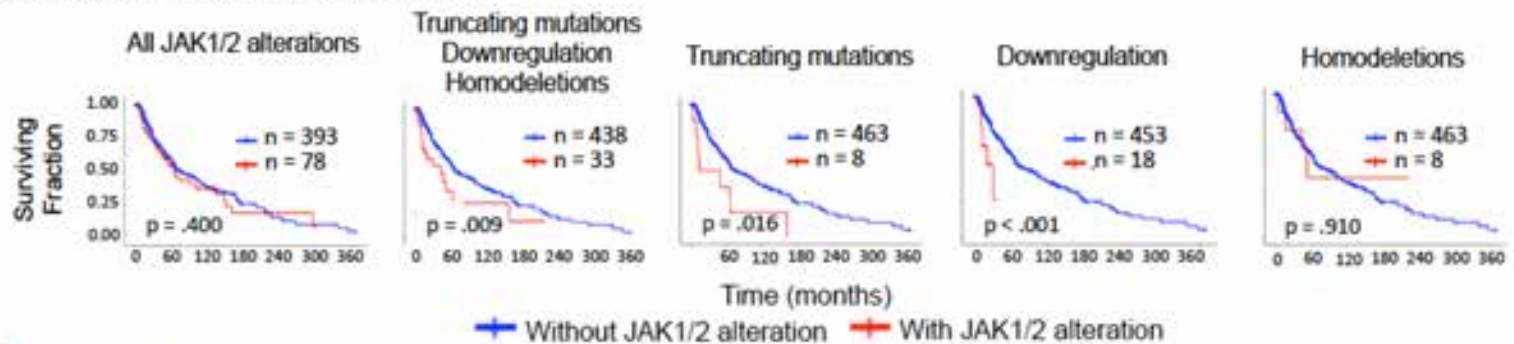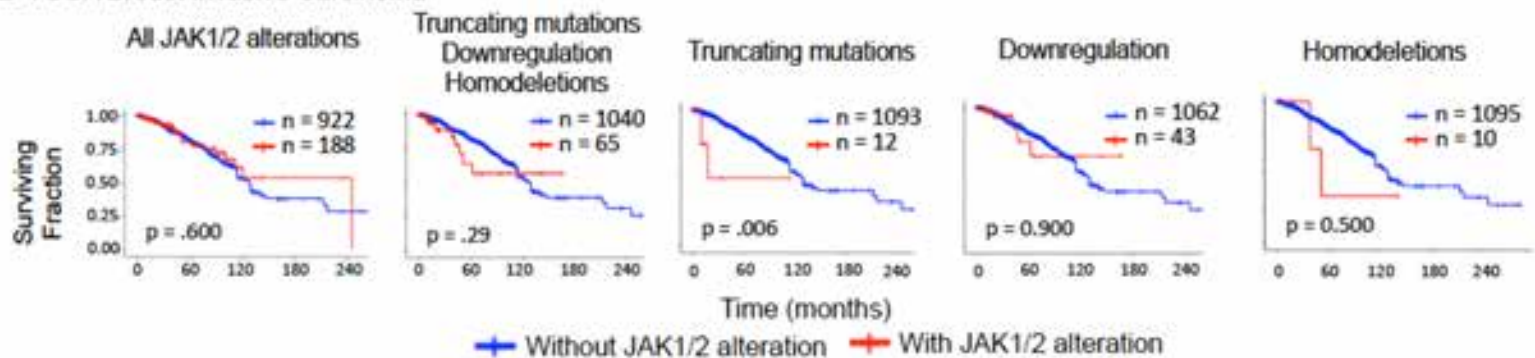# Figure 2

Figure 3

Figure 4

Figure 5

Figure 6

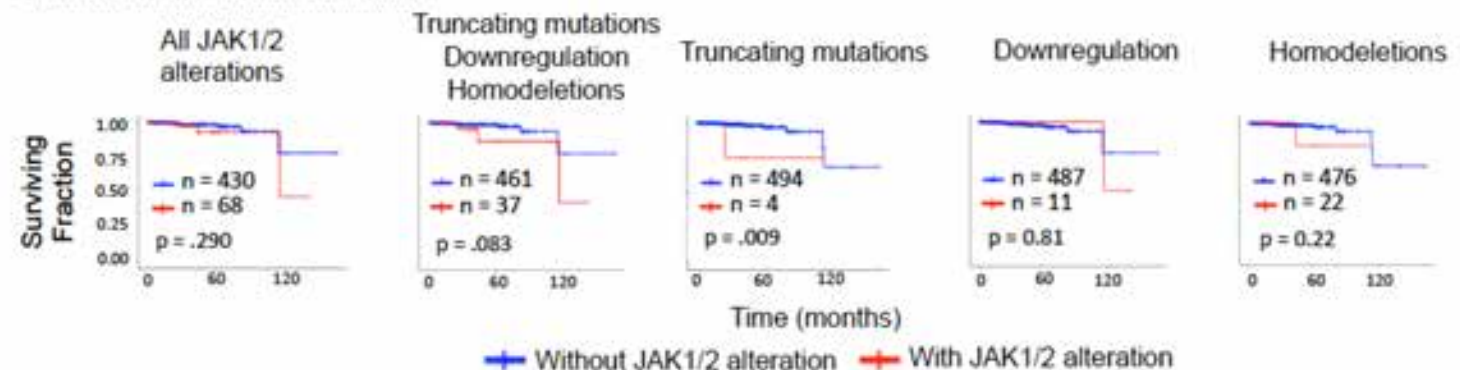A TCGA Skin Subcutaneous Melanoma

B TCGA Breast Invasive Carcinoma

C TCGA Prostate Adenocarcinoma

CANCER DISCOVERY

AACR American Association for Cancer Research

Primary Resistance to PD-1 Blockade Mediated by JAK½ Mutations

Daniel Sanghoon Shin, Jesse M. Zaretsky, Helena Escuin-Ordinas, et al.

Updated version	Access the most recent version of this article at: doi:10.1158/2159-8290.CD-16-1223
Supplementary Material	Access the most recent supplemental material at: http://cancerdiscovery.aacrjournals.org/content/suppl/2016/11/30/2159-8290.CD-16-1223.DC1.html
Author Manuscript	Author manuscripts have been peer reviewed and accepted for publication but have not yet been edited.

E-mail alerts	Sign up to receive free email-alerts related to this article or journal.
Reprints and Subscriptions	To order reprints of this article or to subscribe to the journal, contact the AACR Publications Department at pubs@aacr.org.
Permissions	To request permission to re-use all or part of this article, contact the AACR Publications Department at permissions@aacr.org.